Effect of the Filler Size and Content on the Thermomechanical Properties of Particulate Aluminum Nitride Filled Epoxy Composites

K. C. Yung,[1] B. L. Zhu,[1] T. M. Yue,[1] C. S. Xie[2]

[1]*Department of Industrial and Systems Engineering, Hong Kong Polytechnic University, Hung Hom, Kowloon, Hong Kong, People's Republic of China*
[2]*Department of Materials Science and Engineering, Huazhong University of Science and Technology, Wuhan 430074, People's Republic of China*

Received 9 June 2008; accepted 17 March 2009
DOI 10.1002/app.31431
Published online 1 December 2009 in Wiley InterScience (www.interscience.wiley.com).

ABSTRACT: Polymer matrix composites based on brominated epoxy as the matrix and aluminum nitride (AlN) particles as the filler were prepared. The influences of the size, content, and size distribution of AlN on the thermomechanical properties, including the glass-transition temperature (T_g), coefficient of thermal expansion (CTE), dynamic storage modulus (E'), dynamic loss modulus (E''), and loss factor (tan δ), of the composites were investigated by thermomechanical analysis and dynamic mechanical analysis. There was a total change trend for T_g; that is, T_g of the composites containing nano-aluminum nitride (nano-AlN; 50 nm) was lower than that of the micro-aluminum nitride (micro-AlN; 2.3 μm) filled composites, especially at high nano-AlN contents. The T_g depression of the composites containing nano-AlN was related to the aggregation of nano-AlN and voids in the composites. On the other hand, the crosslink density of the epoxy matrix decreased for nano-AlN-filled composites, which also resulted in a T_g depression. The results also show that E' and E'' increased, whereas tan δ and CTE of the composites decreased, with increasing the AlN content or increasing nano-AlN fraction at the same AlN content. These results indicate that increasing the interfacial areas between AlN and the epoxy matrix effectively enhanced the dynamic modulus and decreased CTE. In addition, at a fixed AlN content of 10 wt %, a low E' of pre-T_g (before T_g temperature) and high T_g were observed at the smaller weight ratio of nano-AlN when combinations of nano-AlN plus micro-AlN were used as the filler. This may have been related to the best packing efficiency at that weight ratio when the bimodal filler was used. J Appl Polym Sci 116: 225–236, 2010

Key words: composites; fillers; glass transition; resins; thermodynamics

INTRODUCTION

To improve the performance of a polymer, the incorporation of inorganic fillers, such as ceramics, carbon black, metals, and metal oxides, has long been an important technique in laboratory research and industrial activity. This method synergistically integrates the advantages of the polymers and inorganic fillers, and the properties of the composites can change with the filler components, geometric shape, particle size, dispersion state, surface properties, particle size distribution, and concentration. It has been established that a micrometer-sized filler (microfiller) can significantly improve the thermal, electrical, and mechanical properties of a pure polymer matrix. In recent years, with the commercial availability of nanoparticles, the use of a nanometer-sized filler (nanofiller) to modify the polymer has been of increasing interest.[1–3] This is because nanofillers with high surface-to-volume ratios will result in increased interfacial area of the polymer and nanofiller and enhanced interaction between them; this can further enhance the properties of the composite. As we expected, the literature shows that nanofillers can more markedly improve the thermal, electrical, and mechanical properties of a composite, such as the strength, modulus, and dimensional stability, compared with microfillers.[1–7] However, unlike microfillers, that usually cause the glass-transition temperature (T_g) of a polymer to increase,[8–11] the effect of nanofillers on the T_g of the polymer matrix is inconsistent. Although the T_g of the polymer can be increased by nanofillers in some cases,[12–15] decreases in T_g,[16–19] no obvious change in T_g,[20,21] and an initial increase in T_g followed by a decrease in T_g with a higher nanofiller content have been also reported.[21,22] Because T_g is a very important property in the determination of the suitability of a polymer for engineering applications, the difference in change trend between T_g's, caused by microfillers

Correspondence to: K. C. Yung (mfkcyung@inet.polyu.edu.hk.).

Contract grant sponsor: Research Grants Council of the Hong Kong Special Administrative Region, China; contract grant number: PolyU5315/05E.

and nanofillers is worthy of investigation. Furthermore, revealing the change rule of T_g for different polymer–filler systems and the underlying mechanisms that govern the T_g phenomenon are necessary and can offer important information for the application of nanofillers.

Except for the effect of filler size, controlling the size distribution of the filler can also optimize the properties of composites; that is, the combined use of two or more than two different size fillers in an appropriate ratio can give the composites better properties than the use of a single-size filler. For example, a binary mixture of an aluminum nitride (AlN) filled (65 vol %) epoxy molding compound showed improved fluidity, thermal conductivity, dielectric constant (D_k), flexural strength, and water resistance compared to an epoxy molding compound filled with single-size particles of AlN;[23] the thermal conductivity of boron nitride (BN)-filled polybenzoxazine exhibited a very high conductivity value as a large particle size with multimodal particle size distribution was used;[24] and a high D_k with a low dissipation factor (D_f) was achieved with the optimized bimodal aluminum-filled composites.[25] However, little research has been reported on the effect of size distribution of the filler on the thermomechanical properties of epoxy composites.[26]

In this study, polymer matrix composites based on brominated epoxy as the matrix and AlN particles as the filler were prepared. AlN possesses a set of excellent properties, such as a high thermal conductivity (319 W/mK), a high electrical resistivity (5×10^{-13} Ω cm), low thermal expansion coefficient (CTE; 4.5 ppm/K), and good mechanical properties at high temperature ranges. The brominated epoxy is widely used in printed circuit board substrates. The addition of AlN will offset some deficiencies of brominated epoxy as substrate materials, such as high CTE, low thermal conductivity, and low strength.[7,27–29] In our previous report, the effect of AlN size on the properties, such as CTE (pre-T_g and post-T_g), D_k, D_f, tensile strength, and Young's modulus, of a brominated epoxy resin were evaluated.[7] However, the very important T_g of the composite was not presented or discussed in detail. In this study, micro-aluminum nitride (micro-AlN) and nano-aluminum nitride (nano-AlN) particles were selected as the fillers. Furthermore, the combined use of nano-AlN and micro-AlN fillers was attempted. When the filler content varied, a micro-AlN plus nano-AlN combination with a fixed weight ratio was used. At a fixed AlN content, a set of weight ratios of nano-AlN were chosen. The effect of the size, content, and weight ratio of nano-AlN in combination with T_g was systemically investigated.

For this study, T_g of the composites was determined by thermomechanical analysis (TMA) and dynamic mechanical analysis (DMA). Associated with these two techniques, some other thermomechanical properties of composites, such as CTE, dynamic storage modulus (E'), loss modulus (E''), and loss factor (tan δ), were also obtained and are discussed in this article.

EXPERIMENTAL

Raw materials

As fillers, micro-AlN and nano-AlN powders were purchased from Hefei Kiln Nanometer Technology Development Co., Ltd. (China), with average sizes of about 2.3 μm and 50 nm, respectively. The coupling agent was 3-glycidoxypropyltrimethoxysilane (trade name KBM-403), purchased from Shin-Etsu Handotai, Ltd. (Japan). The epoxies used as the matrix were Epon 8008 and Epon 1031, purchased from Huntsman Co. (USA). Epon 8008 is a kind of brominated epoxy resin that has been specially designed to meet the stringent requirements of the printed circuit board industry. It has an epoxide equivalent of 410–460 g/equiv and a bromine content of 19.0–21.0% w/w. Epon 1031 is a solid multifunctional epichlorohydrin/tetraphenylol ethane epoxy resin with an epoxy group content of 4350–5130 mmol/kg. Epon 1031 is used to improve the properties of cured epoxy resin systems, particularly at elevated temperatures. In this study, Epon 8008 and Epon 1301 were dissolved in acetone, and their contents in the solution were 80 and 70% w/w, respectively. The curing agent dicyandiamide (DICY; purity > 99.5%) and the accelerator 2-methylimidazole (2-MI; purity > 99.0%) were obtained from Neuto Products (China) and Tokyo Kasei Kogyo, respectively. The DICY particles had an average diameter of less than 1 mm. DICY and 2-MI were used as received.

Procedure for composite preparation

The epoxy–AlN composites were fabricated according to the following steps:

1. The surface of the AlN powder was pretreated with a KBM-403 coupling agent, with the amount used being 5 wt % on the basis of the weight of the AlN powder.
2. Epon 8008 solution, Epon 1031 solution, DICY, 2-MI, and AlN were weighed at a certain ratio, as listed in Table I.
3. The mixtures, diluted by a small quantity of acetone, were first stirred in a beaker for 45 min by an ultrasonic stirrer, and then, they were stirred by a high-speed mixing machine for 1 h.
4. The uniformly formed mixtures were cast in a mold and were pumped for about 1 h to remove the air bubbles and solvent as the temperature was gradually increased from 80 to 130°C.

TABLE I
Basic Recipe of the Epoxy–AlN Composites

Material	Ratio of materials by weight
Epon 8008 solution	100
Epon 1301 solution	7.349
DICY	2.552
2-MI	0.056
AlN	0–40

5. Finally, the mixtures were heated to 175°C for 4 h to complete polymerization.

When the filler content was varied from 2.5 to 40 wt %, single micro-AlN and nano-AlN fillers were first chosen, respectively, and then, a micro-AlN plus nano-AlN filler combination with a weight ratio of 1 : 1 was used. To further study the effects of filler size distribution on the properties of the composites, at a fixed AlN content of 10 wt %, a set of weight ratios of nano-AlN [Nano-AlN/(Micro-AlN + Nano-AlN)], that is, 0, 0.17, 0.33, 0.5, 0.67, 0.83, and 1, were chosen.

Characterization

Density measurement

The density of the epoxy–AlN composites was measured by the Archimedes principle with alcohol as the medium. The theoretical densities of the composites were calculated on the basis of the density of AlN of 3.26 g/cm^3 and the measured density of the epoxy. The volume percentage of filler was determined from the densities of the neat epoxy and filler.

TMA

CTE and T_g were measured with a PerkinElmer (USA) thermomechanical analyzer (TMA-7). The temperature range used was 30–220°C, and the heating rate was 10°C/min. All reported TMA data were obtained from a second heating cycle.

DMA

DMA was carried out for the composites with a dynamic mechanical thermal analyzer (PerkinElmer Diamond DMA Lab System) at frequencies of 0.1, 1, 5, 10, and 50 Hz from 30 to 200°C at a heating rate of 3°C/min. The dynamic modulus and tan δ values were obtained in tensile mode. T_g was also determined by DMA.

Scanning electron microscopy (SEM) analysis

A field emission scanning electron microscope (JEOL, JSM-6335F, Japan) was used to analyze the fracture surfaces of the epoxy–AlN composites. A thin section of the fracture surface was mounted on an aluminum stub with a conductive (silver) paste and was coated with gold before fractographic examination.

RESULTS AND DISCUSSION

Density and volume percentage

Table II shows the measured density and theoretical density values of the composites with different AlN contents and the volume percentage of the AlN filler in the composites. As shown in Table II, the theoretical density was higher than the measured density regardless of the use of micro-AlN, nano-AlN, or their combination filled composites. Compared with the theoretical density, the measured densities of the micro-AlN-filled composites slightly decreased, but those of the nano-AlN-filled composites greatly decreased. The measured value of the micro-AlN plus nano-AlN filled composites was between that of the micro-AlN-filled and nano-AlN-filled composites. Table III shows the measured density of the composites filled with the 10 wt % combination of micro-AlN plus nano-AlN with different weight ratios of nano-AlN. These values were still lower than the theoretical values, and they were also between those of the micro-AlN-filled and nano-AlN-filled composites.

Because the measured density of neat epoxy was regarded as the theoretical value, that is, the neat epoxy was supposed to be void free, when the theoretical density was higher than the measured density, this indicated that the AlN filler brought out some

TABLE II
Measured Density and Theoretical Density of the Composites with Different AlN Contents

	Measured density (g/cm^3)				
AlN (wt %)	Micro-AlN	Nano-AlN	Micro-AlN plus nano-AlN	Theoretical density (g/cm^3)	Volume percentage of the AlN filler (%)
0	1.3846	–	–	–	0
2.5	1.4142	1.3976	1.3922	1.4070	1.20
5	1.4240	1.4163	1.4160	1.4289	2.36
10	1.4700	1.4483	1.4519	1.4712	4.62
20	1.5424	1.5129	1.5384	1.5501	8.83
40	1.6823	1.6618	1.6449	1.6888	16.22

TABLE III
Measured Density of the Composites Filled with a 10 wt % Combination of Micro-AlN Plus Nano-AlN with Different Weight Ratios of Nano-AlN

Nano-AlN/ (Micro-AlN + Nano-AlN)	0.17	0.33	0.67	0.83
Measured density (g/cm^3)	1.4508	1.4502	1.4424	1.4535

voids in the composite. The voids originated from air bubbles and/or solvent evaporation. Although the mixture was pumped for a long time to remove the air bubbles and solvent at a high temperature during the preparation of the samples, as mentioned previously, it became difficult to completely remove the bubbles and solvent because the viscosity of the mixture gradually increased with the addition of the AlN filler. Obviously, the viscosity of the mixture increased with increasing AlN filler content. At the same time, the obvious difference in the density between the nano-AlN-filled and micro-AlN-filled composites implied that the viscosity of the mixture also depended on the interfacial area between the filler and the epoxy. At a fixed AlN content, the nano-AlN-filled composite had a large surface area, namely, a large interfacial area between the filler and the epoxy, which induced a high viscosity.[25] The removal of air bubbles and solvent was more difficult because of the high viscosity.[15,25] Finally, reserved bubbles and solvent formed the voids in the composites; thus, the density of the composites decreased. In fact, we found that macroscopic voids sometimes appeared at the sample edge for the nano-AlN-filled composites, and poor moldability was observed as the nano-AlN content was increased to 20 wt %. These phenomena reflected the fact that the nanofiller markedly increased the viscosity of the mixture. When bimodal fillers were used, a minimum viscosity of the mixture was achieved at a suitable bimodal filler ratio, and it usually corresponded to the maximum packing fraction (MPF) of the filler.[23,25,30,31] The theoretical analysis of MPF and the viscosity measurement of the bimodal filler showed that the suitable ratio was 0.2–0.3. However, a remarkable decrease in the viscosity with control of the bimodal filler ratio was observed only at high filler contents. In this study, the volume percentage of AlN in the composites was small (4.62%), and the viscosity may not have been affected by the weight ratio of the nano-AlN. Thus, the density of the composites was not obviously improved (Table III).

T_g

Figure 1 shows T_g of the TMA of the composites as a function of the AlN content. T_g of the composites gradually increased with increasing micro-AlN content. When the nano-AlN filler was used, T_g increased slightly as the filler content increased to 10 wt %, and thereafter, it began to decrease. The change trend of T_g with filler content for the nano-AlN plus micro-AlN filled composites was the same as for the nano-AlN-filled composites, but the value was between that of the nano-AlN-filled and micro-AlN-filled composites. Figure 2 shows T_g as a function of the weight ratio of nano-AlN in the combination of micro-AlN plus nano-AlN for the composites with 10 wt % AlN. The results show that T_g first increased and then decreased with the weight ratio of nano-AlN. The maximum T_g was obtained at a weight ratio of nano-AlN of 0.33.

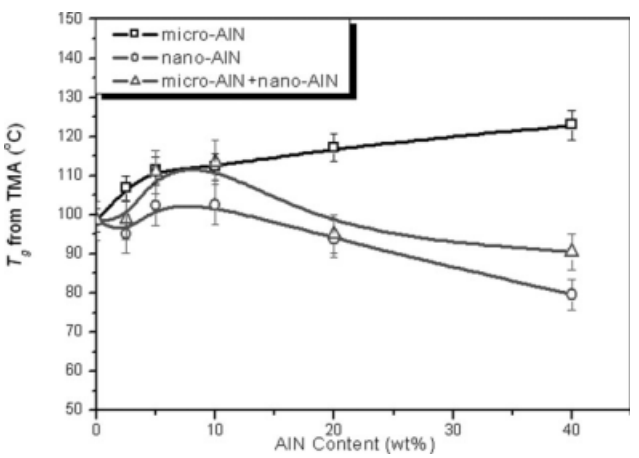

Figure 1 Relationship between the T_g (measured by TMA) and AlN content.

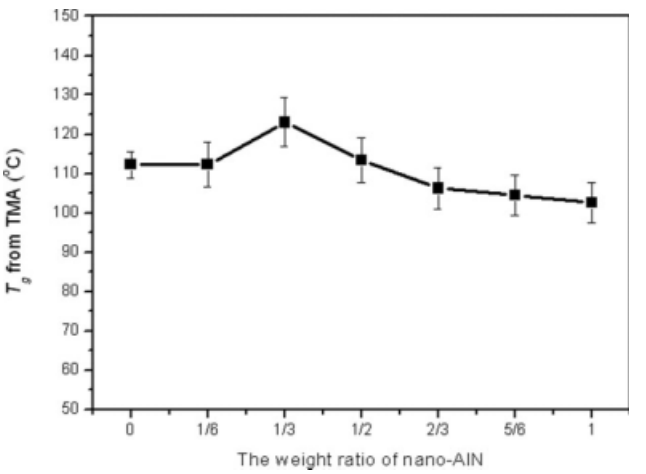

Figure 2 T_g (measured by TMA) as a function of the weight ratio of nano-AlN in the combination of micro-AlN plus nano-AlN for the composites with 10 wt % AlN.

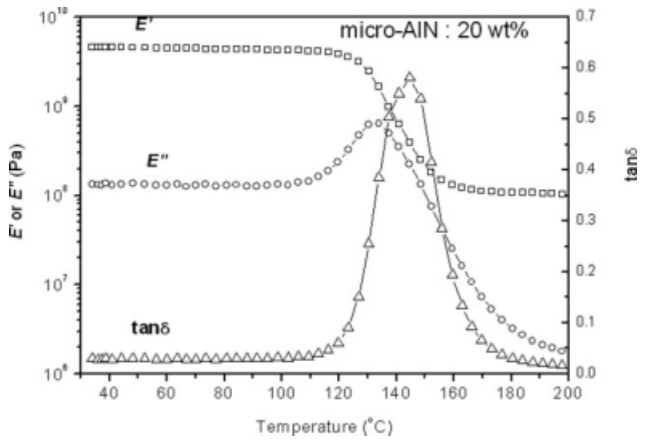

Figure 3 Typical E', E'', and tan δ versus T curves for the 20 wt % micro-AlN-filled epoxy at a testing frequency of 1 Hz.

T_g could also be obtained by DMA, and the typical DMA curves, that is, temperature dependence of E', E'', and tan δ, are shown in Figure 3. In the curves of E', E'', and tan δ versus T (temperature) around a certain temperature region, there were some significant differences, such as a steep decrease in E' and a peak appearing in the E'' and tan δ curves, which is a typical feature of glass transition. The values of T_g from the tan δ versus T curves at a testing frequency of 1 Hz for the different contents AlN-filled epoxy are shown in Figure 4. Figure 5 shows the values of T_g from the tan δ versus T curves at a testing frequency of 1 Hz as a function of the weight ratio of nano-AlN in the combination of micro-AlN plus nano-AlN for the composites with 10 wt % AlN. The change trend with the AlN content of T_g from DMA was consistent with that from TMA. However, it was slightly different from the TMA results that the T_g value showed fluctuation with the weight ratio of nano-AlN, and a high

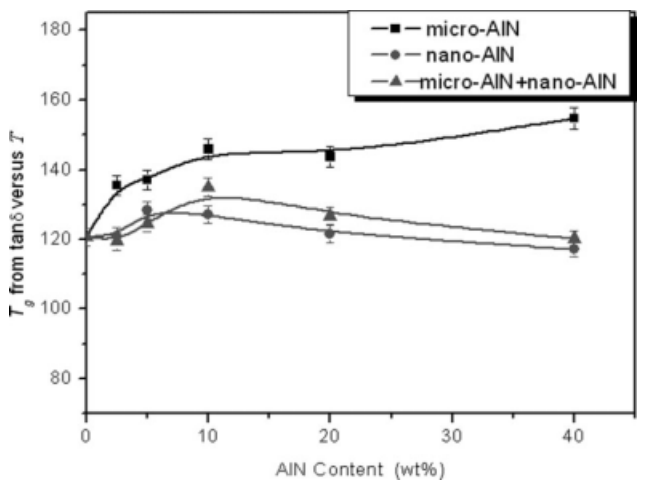

Figure 4 T_g from the tan δ versus T curves at a testing frequency of 1 Hz as a function of AlN content.

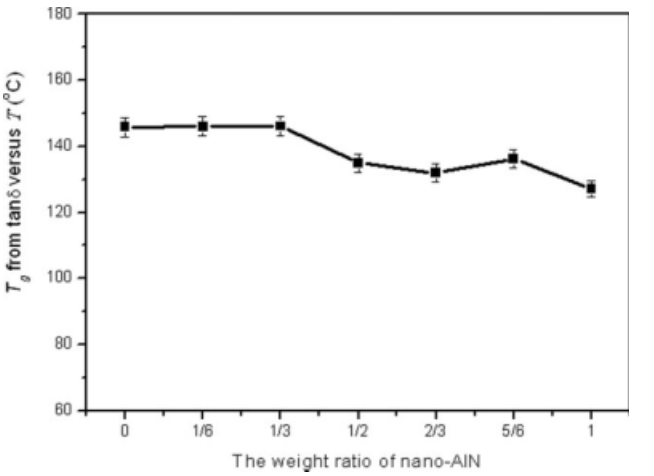

Figure 5 T_g determined from the tan δ versus T curves at testing frequency of 1 Hz as a function of the weight ratio of nano-AlN in the combination of micro-AlN plus nano-AlN for the composites with 10 wt % AlN.

T_g was observed at lower weight ratios of nano-AlN (0.17–0.33). Kwon et al.[26] also found that T_g was higher at lower weight ratios of smaller sized silicates (0.2–0.5). The differences between the T_g values measured by TMA, DSC, and DMA were also reported by other researchers.[32]

T_g from DMA was affected by the testing frequency. T_g increased with increasing testing frequency. The glass transition of the polymer is a molecular relaxation that involves cooperative segmental motion, the rate of which depends on temperature.[33] The molecules at high frequencies do not have time to undergo relaxation compared with the molecules at low frequencies. However, with increasing temperature, molecular relaxation at high frequencies occurs because of the increase in the rate of molecular relaxation. Thus, T_g increased with an increase in testing frequency. On the basis of the modified Arrhenius equation, the activation energy (ΔE) of the glass transition can be calculated:[34]

$$\ln \omega = \ln \omega_0 - \frac{\Delta E}{RT_g}$$

where ω is the testing frequency, ω_0 is the constant characteristic of the materials, T_g is the glass-transition temperature from the tan δ versus T curve, and R is the universal gas constant. Values of ΔE can be obtained from the linear regression of ln ω versus $1/T_g$. Figure 6 shows ΔE as a function of AlN content. The change trend in ΔE with AlN content was easily found to be the same as T_g. A high T_g implied that the mobility of the chain was relatively difficult, as discussed later, and thus, ΔE of the glass transition increased.

As mentioned in the Introduction, the effect of the filler in polymer composites on the glass-transition

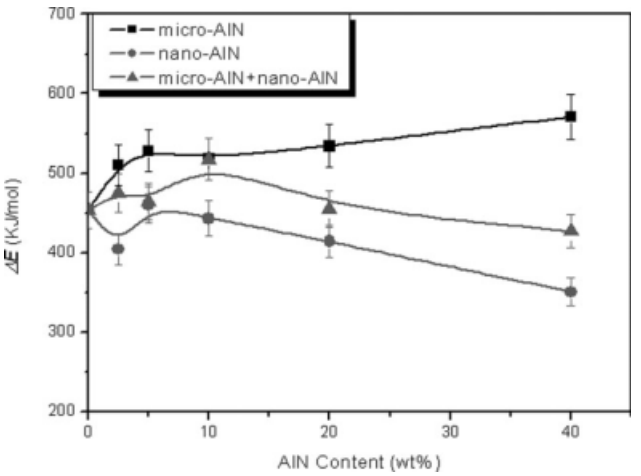

Figure 6 ΔE of glass transition as a function of AlN content.

behavior of the polymer matrix has been studied for different polymer–filler composites. The addition of a microfiller usually increases the T_g of the composites. This implies that the chain mobility is restricted because of the presence of a microfiller.[8–11] For the nanofiller, some researchers have found that T_g of composites increased as a function of the filler content, and the increase in T_g was also ascribed to the restriction of the chain mobility due to the interaction of epoxy and filler.[12–15] Although different reasons supported by researchers, including the crosslink density and amount of reaction residue, have been used to explain the T_g depression of nanocomposites, the increase in the chain mobility is the most direct reason for the depression.[16–19] As the filler size decreases, the interfacial area between the fillers and the polymer matrix increases dramatically. If the interaction between the polymer matrix and the nanofiller is strong, the mobility of the chain can be effectively restricted, and this, thus, increases T_g.[35] To obtain the strong interaction between the polymer and the nanofiller, dispersion, and compatibility with the polymer of nanofiller are very important. Good dispersion and/or compatibility with the polymer of the nanofiller, obtained by the application of special dispersion technology and surface modification of the nanofiller with a coupling agent, can enhance the T_g.[13,22,30,36] The aggregation of the nanofiller and poor compatibility with the polymer will result in a weak interaction between the nanofiller and the polymer. Weak interaction between the filler and polymer implies that more free volume exists at the filler–polymer interface, thus, it cannot effectively confine the mobility of the polymer chain. At the same time, the aggregation of the nanofiller and poor compatibility with the polymer easily induce voids in the composites. As a result, the polymer chain shows a relatively high mobility, and thus, the glass transition is completed at a lower temperature. Generally, it is difficult to disperse the nanofiller, especially at high nanofiller contents, and thus, the aggregation of the nanofiller easily forms. On the other hand, the surface of the nanofiller can easily absorb some molecules, such as water and organics, because of its large surface area during preparation and conservation. The adsorbed water, together with other bonded surface organics, is not compatible with the polymer matrix.[21] In conclusion, the T_g depression is related to weak interaction, which is caused by the aggregation of the nanofiller, poor compatibility with the polymer, and voids in the composites.

For this study, the fracture surfaces of the composites were observed by field emission SEM to analyze the distribution state of AlN in the composites and the interface state between the epoxy and AlN. Figure 7 shows the fracture images of the composites containing different AlN sizes and contents. For the micro-AlN-filled composites, less AlN filler was obviously exposed on the surface, and thus, it was difficult to distinguish the AlN filler and epoxy matrix, as shown in Figure 7(a–c). This was related to the fact that the number of AlN molecules per unit area for the micro-AlN-filled composites was much smaller than that for the nano-AlN-filled composites. On the other hand, this also indicated good compatibility and strong interaction between the micro-AlN and the epoxy, and thus, it was difficult to peel off the AlN from the epoxy matrix. As shown in Figure 7(b), the AlN was coated by epoxy, and there was a strong interfacial adhesion between them. The interaction between micro-AlN and the epoxy effectively inhibited the mobility of the epoxy chain, and this effect was enhanced with increasing AlN content. Thus, T_g gradually increased with increasing micro-AlN content. When the nano-AlN was used, AlN exposed on the fracture surface was easily observed, even when the AlN content was small (2.5 wt %), as shown in Figure 7(d–j). As shown in Figures 7(d), 7(g), and 7(i), the AlN exposed on the surface formed aggregations. Some voids (pointed out by arrows) were seen in the magnified images of these aggregations (marked by ellipses) of nano-AlN, as shown in Figures 7(e), 7(h), and 7(j). Obviously, the interaction between these aggregations of nano-AlN and the epoxy matrix was relatively weak; thus, nano-AlN was easily peeled from the epoxy matrix and exposed on the surface. However, it is worth noting that the interaction of nano-AlN and the epoxy matrix in some regions remained strong, which was also indicated by the epoxy coating AlN and the strong interfacial adhesion between them. As a small amount of nano-AlN was filled, the amount of aggregation and voids were small, and the decrease in the mobility of the chain caused by the interaction

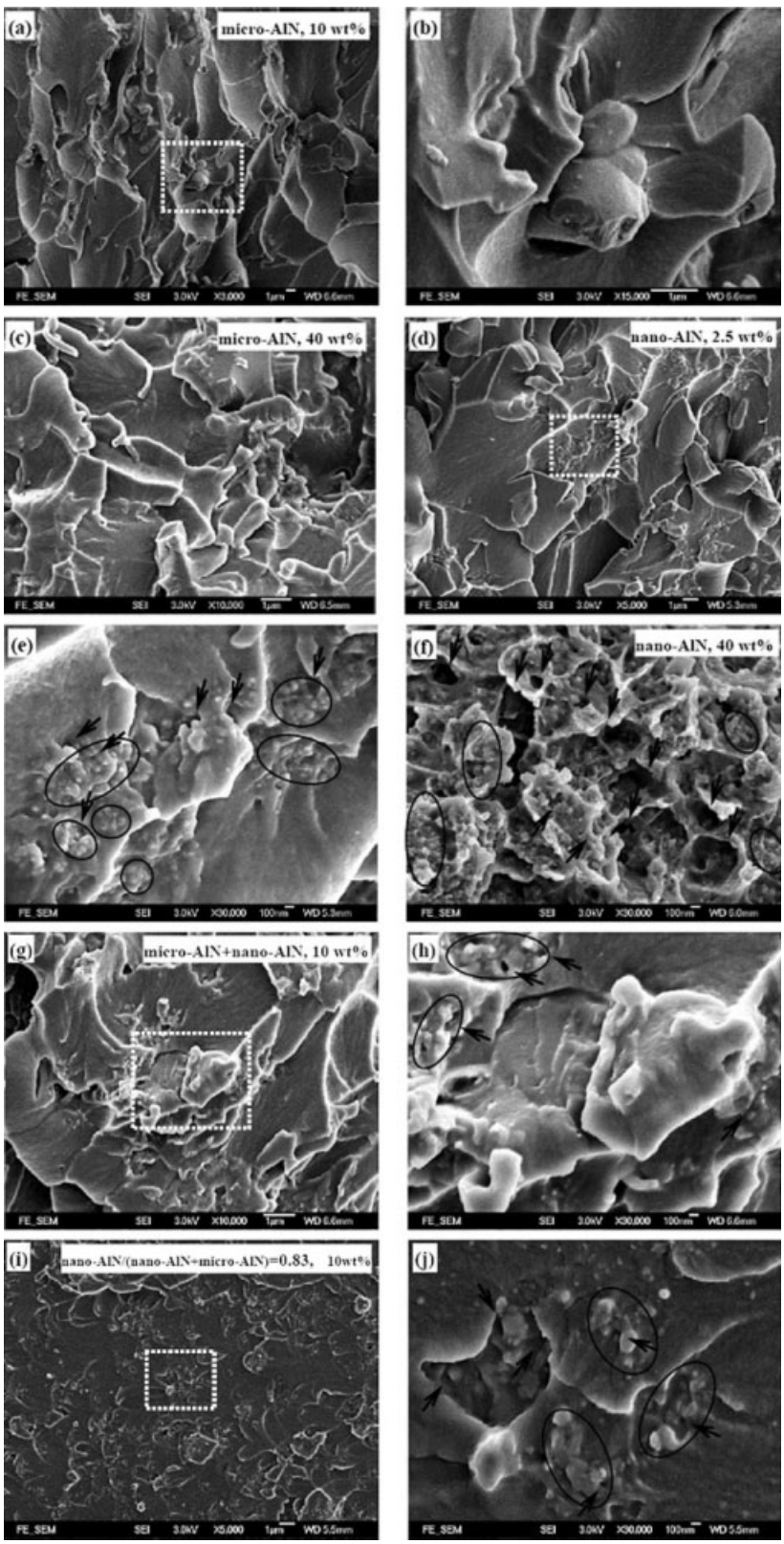

Figure 7 SEM images of the fracture surfaces of the composites containing different AlN sizes and contents: (a) micro-AlN, 10 wt %; (b) magnified image of the marked square in (a); (c) micro-AlN, 40 wt %; (d) nano-AlN, 2.5 wt %; (e) magnified image of the marked square in (d); (f) nano-AlN, 40 wt %; (g) micro-AlN plus nano-AlN, 10 wt %; (h) magnified image of the marked square in (g); (i) Nano-AlN/(Nano-AlN + Micro-AlN) = 0.83, 10 wt %; and (j) magnified image of the marked square in (i).

between them may have been stronger than the increase in the mobility of chain because of the existence of the aggregation of nano-AlN and voids. Finally, T_g increased with a small increase in nano-AlN, but the increase was smaller than that of micro-AlN. With further addition of nano-AlN, it became more difficult to disperse nano-AlN and remove bubbles and solvent because of the increased viscosity; thus, more aggregations of nano-AlN and voids existed in the composite [Fig. 7(f)], which greatly improved the mobility of the epoxy chain. As a result, T_g decreased at high nano-AlN contents. Compared with a single micro-AlN, T_g was smaller because of the existence of nano-AlN in the composite when the micro-AlN plus nano-AlN were used as fillers. However, at the same time, T_g was larger than that of a single nano-AlN-filled composite because the actual amount of nano-AlN in the composite was smaller than that of the single nano-AlN-filled composite. Also, the gradual increase in the actual amount of nano-AlN in the composite caused T_g to first increase and then decrease with increasing AlN content. This implied that the effect of nano-AlN in combination of micro-AlN plus nano-AlN was remarkable and dominant.

According to SEM analysis, T_g of the composite was strongly dependent on the microstructure of the composite. In addition, the T_g depression with nano-AlN may have been related to the reduction of the crosslink density of the epoxy matrix because of the increase in the viscosity induced by the nano-AlN during composite preparation.[18]

At a fixed AlN content of 10 wt %, a high T_g was observed at weight ratios of nano-AlN of 0.17–0.33; these were close to the ratio corresponding to the MPF of filler (0.2–0.3), as mentioned previously. This implies that a high T_g was related to the MPF of the filler when the bimodal fillers were used. The thermal conductivity and dielectric properties can be greatly improved by the best packing efficiency.[23–25] However, the best packing efficiency was not very obvious in this study because of the small volume percentage of AlN in the composite (4.62%). An obvious improvement in T_g due to the best packing efficiency was more clearly observed in the composites with a high AlN volume percentage.

Coefficient of thermal expansion (CTE)

CTEs of the AlN-filled epoxy composites were examined with TMA. Figure 8(a) shows that CTE of pre-T_g of the composite varied with the AlN content. CTE of the composites obviously decreased as the filler content increased. However, the decreased extent depended on the filler size. At the same filler content, the order of decreased extent in CTE of the composites was Nano-AlN > Nano-AlN plus micro-AlN > Micro AlN. Figure 8(b) shows the CTE of post-T_g (temperature after glass transition temperature) of the composite as a function of the AlN content. Also, the degree of decrease differed according to the AlN sizes and contents. CTE of post-T_g also decreased with increasing AlN content, but the dependence of CTE of post-T_g on the AlN size was the reverse that of pre-T_g; that is, the order of decreased extent in CTE of post-T_g was Micro-AlN > Nano-AlN plus micro-AlN > Nano-AlN. Figure 9 shows the CTE of pre- and post-T_g as a function of the weight ratio of nano-AlN in the combination of micro-AlN plus nano-AlN for the composites with 10 wt % AlN. CTEs of pre-T_g and post-T_g for the composites with different weight ratios of nano-AlN were 52–57 and 176–184 ppm/°C, respectively. There was a total trend; that is, CTE of pre-T_g increased and CTE of post-T_g decreased with increasing weight ratio of nano-AlN; this was consistent with the results of the single nano-AlN- and micro-AlN-filled composites.

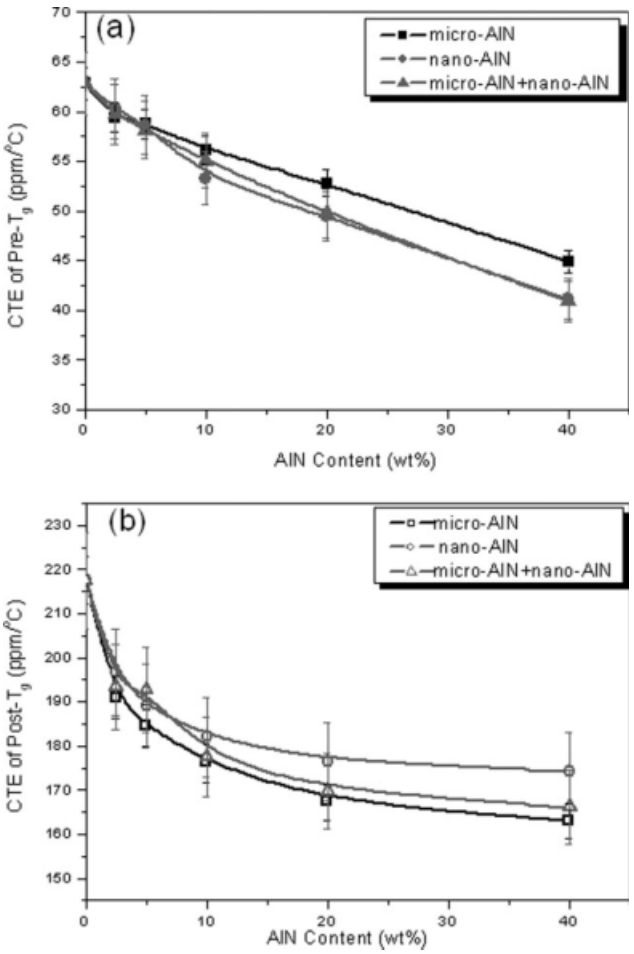

Figure 8 CTE of (a) pre-T_g and (b) post-T_g of the composites as a function of AlN content.

Dynamic modulus

E' of pre-T_g and post-T_g, that is, in the glassy state and rubbery state, were not constant, but they

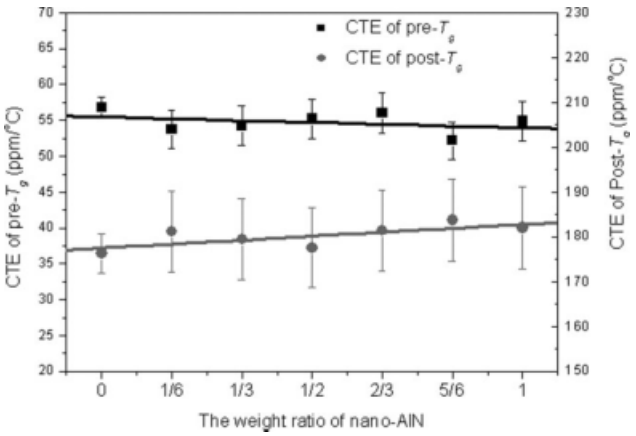

Figure 9 CTE of pre-T_g and post-T_g as a function of the weight ratio of nano-AlN in the combination of micro-AlN plus nano-AlN for the composites with 10 wt % AlN.

slightly decreased with temperature, as shown in Figure 3. This decrease in E' with temperature in the glassy and rubbery regions may have been due to the different CTEs of the matrix and filler inducing relaxation in the polymeric phase.[18] In the glassy or rubbery region, E'' almost remained constant compared with E'. Thus, the E' and E'' values taken at about 30 and 200°C were assumed as E' and E'' in the glassy and rubbery states, respectively. The values of E' in the glassy and rubbery states are shown in Figure 10(a,b), respectively. E' showed a monotonic increasing trend with AlN content. E' was also dependent on the AlN size. At the same AlN content, E' of the nano-AlN-filled composites was larger than that of the micro-AlN-filled composites in the glassy state, but it was the reverse in the rubbery state. The values of E' for the micro-AlN plus nano-AlN-filled composites were between those of micro-AlN- and nano-AlN-filled composites in both states. These change trends of E' were consistent with CTE. CTE of AlN was much lower than that of epoxy, and the elastic modulus of AlN was much higher than that of epoxy; thus, the deformation of the composites was hindered by AlN to result in a decrease of CTE and an increase in E' with an increase in AlN content. Compared with micro-AlN, nano-AlN had a higher surface area, which implied that more interfacial area formed between nano-AlN and the epoxy, even with the existence of the aggregation of nano-AlN. Thus, nano-AlN could more effectively restrict the deformation of the epoxy matrix, although the interaction of the epoxy and nano-AlN was weak in some regions because of the aggregation of nano-AlN and voids, as discussed previously. As a result, CTE of the nano-AlN-filled composites was lower, and E' was higher compared with that of the micro-AlN-filled composites. In fact, a weak interaction between the filler and polymer may have resulted in a decrease of T_g, but increased E' by hindering the macroscopic deformation of the polymer matrix. Thus, a decrease in T_g and an increase in E' with nanofiller content were observed at the same time by many researchers.[16–19] A higher CTE and lower E' than in the micro-AlN-filled composites in the rubbery state was found for the nano-AlN-filled composites. This may have been related to the decrease in crosslink density of the epoxy matrix for the nano-AlN-filled composites. Miyagawa and Drzal[17] found that E' of fluorinated single-walled carbon nanotubes (FSWCNT)-filled epoxy nanocomposites increased with FSWCNT contents below T_g, but it decreased with FSWCNT content above T_g. The decrease in E' indicated the decrease in the crosslink density of the anhydride-cured epoxy matrix of FSWCNT nanocomposites, caused by nonstoichiometry due to the addition of FSWCNT.[17] In this study, the reduction in the crosslink density of the epoxy matrix may have been due to the huge viscosity induced by the nano-AlN during composite preparation, as mentioned previously. Furthermore, the deformation of the epoxy matrix became larger because of the decrease in crosslink density, especially in the rubbery state. Thus, we observed a

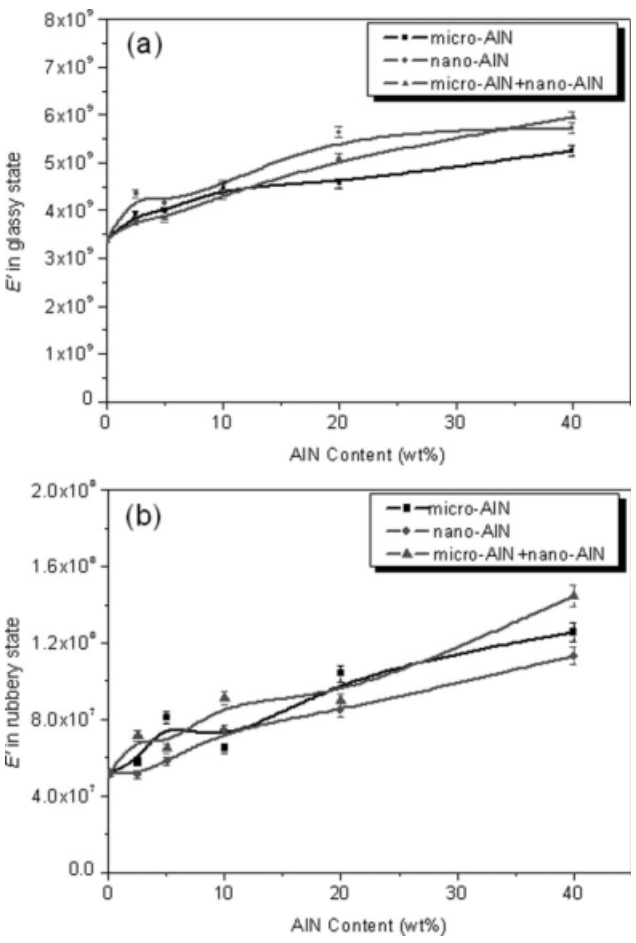

Figure 10 E' in the (a) glassy and (b) rubbery regions of the composites as a function of AlN content.

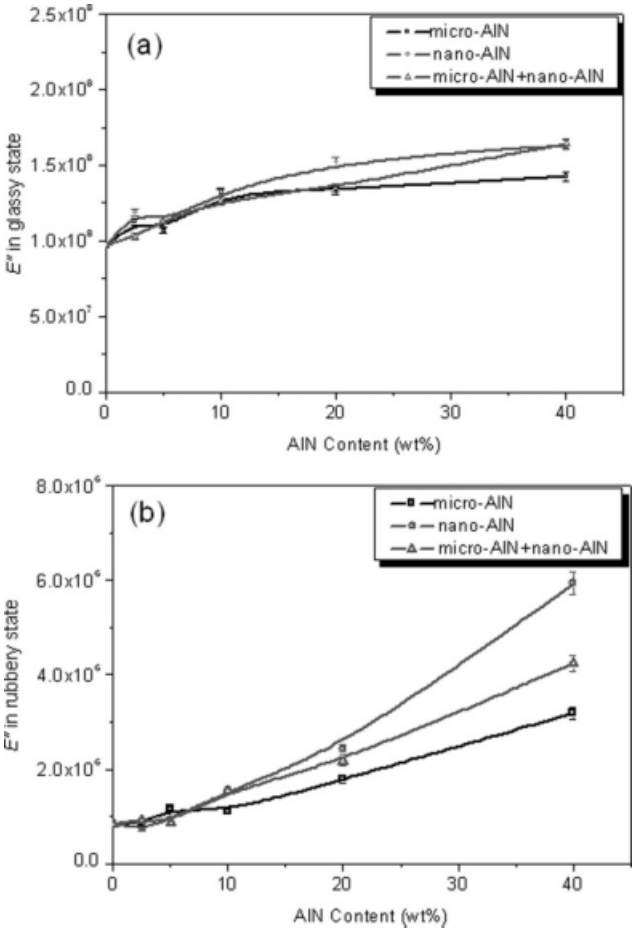

Figure 11 E'' in the (a) glassy and (b) rubbery regions of the composites as a function of AlN content.

higher CTE and lower E' in the rubbery state for the nano-AlN-filled composites at the same AlN content. In addition, as shown Figure 10, the increased percentage E' in the rubbery region was higher than that in the glassy region. For example, as the filled micro-AlN content gradually increased to 40%, the increases in E' in the glassy and rubbery states were about 54 and 142%, respectively.

Figure 11 shows the values of E'' in the glassy and rubbery states as a function of the filler content. Also, E'' of the composites increased as the AlN content increased. Both in the glassy and rubbery states, E'' of the nano-AlN-filled composites was larger than that of the micro-AlN-filled composites, and E'' of the nano-AlN plus micro-AlN-filled composites was between that of the micro-AlN- and nano-AlN-filled composites at the same AlN content. The interfacial area between the matrix and AlN increased with increasing AlN content and/or decreasing AlN size. Therefore, the friction between the matrix and AlN fillers increased correspondingly under the action of outside vibration load and resulted in increasing energy losses.[37] Thus, the value of E'' increased with increasing AlN content and decreasing AlN size. As shown in Figure 11, the increased percentage of E'' in the rubbery region was obviously higher than that in the glassy region, just the same as the E', which indicated that the reinforcing effect of the filler was higher in the rubbery state than in the glassy one. Other authors also observed this phenomenon and provided possible explanations.[11,18,33]

Figure 12 shows E' in the glassy and rubbery regions as a function of the weight ratio of nano-AlN in the combination of micro-AlN plus nano-AlN for the composites with 10 wt % AlN. As shown in Figure 12, the changes in E' and E'' were irregular, but they showed an increasing trend with increasing nano-AlN ratio. Kwon et al.[27] discussed the effect of the size distribution of silica particles on the thermoviscoelastic properties of composites and found that the thermoviscoelasticity was affected by the MPF of silica particles below T_g. When the weight ratio of smaller sized silica was 0.2, MPF was reached, and the minimum E' was obtained at the same time. In this study, the minimum E' in the glassy state was found at a weight ratio of nano-AlN of 0.17, close to 0.2.

Tan δ

Figure 13 shows the tan δ of the composites as a function of AlN content. With increasing filler content, tan δ decreased, despite AlN size, as shown in Figure 13. This implied that the increase in energy dissipation was lower than the stored energy under the action of an outside dynamic load with increasing AlN content; this, correspondingly, decreased the mechanical damping of the composite. Also, tan δ of the nano-AlN-filled composites was minimum and that of the nano-AlN plus micro-AlN-filled composites was maximum at the same AlN content. This difference is not completely understood at present.

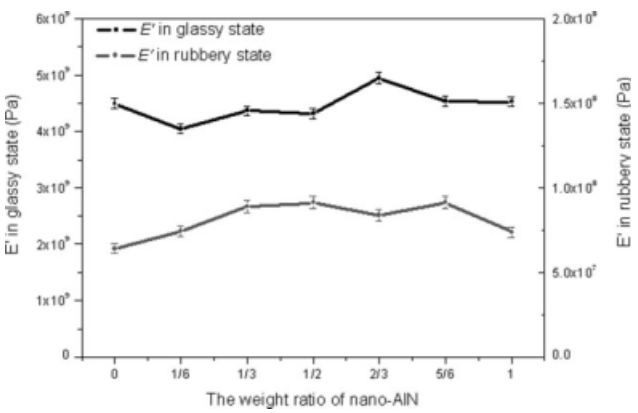

Figure 12 E' in the glassy and rubbery regions as a function of the weight ratio of nano-AlN in the combination of micro-AlN plus nano-AlN for the composites with 10 wt % AlN.

In addition, the width of tan δ increased with increasing AlN content. The peak factor (τ) is defined as the full width at half maximum of the tan δ peak divided by its height and can be qualitatively used to assess the homogeneity of the epoxy network.[13,38] As shown in Figure 14, the neat epoxy was observed to have a low τ; this indicated that the crosslink density and homogeneity of the epoxy network were high. For the AlN-filled composites, τ increased with AlN content. At the same AlN content, τ of the nano-AlN-filled composites was obviously larger than that of the micro-AlN- and micro-AlN plus nano-AlN-filled composites, especially at high AlN content. This indicated that the crosslink density of the epoxy matrix decreased with the addition of nano-AlN, as stated previously.

From the previous results and discussion, we determined that the properties of the composites were strongly dependent on the AlN–epoxy interaction. Generally, the nature of the interface between the organic and inorganic components is divided into two different classes.[39] Class I corresponds to systems in which there are no covalent or ionic–covalent bonds between the organic and inorganic components. There are only Van der Waals forces, hydrogen bonds, or electrostatic forces between them. In contrast, some organic and inorganic components are linked through strong chemical bonds (covalent or ionic–covalent), which are defined as class II materials. In this epoxy–AlN system, the interfacial interactions included class I and II interactions, but which class was had the greater number may have been related to the AlN size and content. Class I interactions in the composites containing nano-AlN were greater than those in the micro-AlN-filled composites, especially at high nano-AlN content. For the micro-AlN-filled composites, the higher interfacial interaction may have been class II. The strong interaction between AlN and the epoxy effectively inhibited the mobility of the epoxy chain, but weak interactions between them may have increased the mobility of the epoxy chain.[21] Thus, T_g of the composites containing nano-AlN (50 nm) was lower than that of the micro-AlN (2.3 μm)-filled composites, especially at high nano-AlN content. However, both strong and weak interactions between AlN and the epoxy effectively restricted the deformation of the epoxy matrix. Thus, increasing the AlN content or increasing the nano-AlN fraction at the same AlN content made E' and E'' increase, whereas tan δ and CTE of the composites decreased.

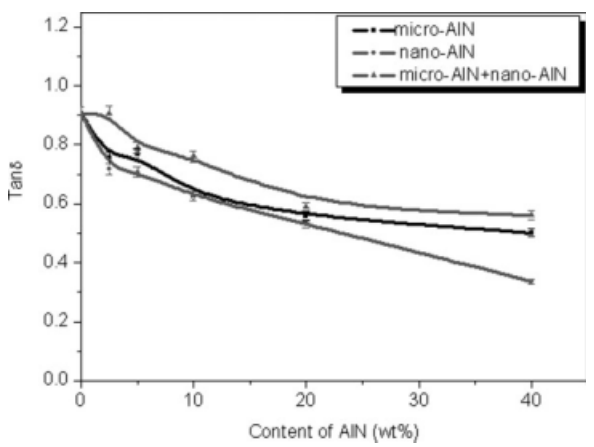

Figure 13 Tan δ of the composites as a function of AlN content.

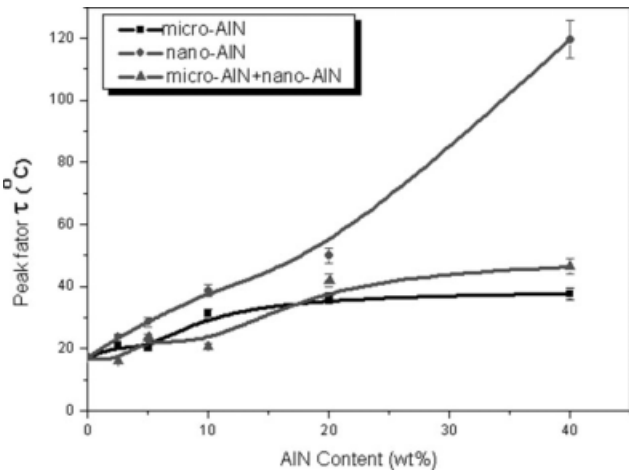

Figure 14 τ of the composites as a function of AlN content.

CONCLUSIONS

1. T_g of the micro-AlN-filled composites gradually increased, but T_g of the nano-AlN-filled composites increased initially and then decreased with increasing AlN content. E' and E'' of the composites increased, and CTE and tan δ of the composites decreased with increasing AlN content.
2. At the same AlN content, CTE of the pre-T_g, E' of pre-T_g, and E'' of nano-AlN-filled composites were higher than those of the micro-AlN-filled composites, but T_g, CTE of post-T_g, and E' of post-T_g were lower than those of the micro-AlN-filled composites.
3. Generally, the values of E', E'', CTE, and T_g of the micro-AlN plus nano-AlN-filled composites were between those of the micro-AlN- and nano-AlN-filled composites, and the change trend of T_g with AlN content was consistent with the nano-AlN-filled composites.
4. From SEM observation, we found that the T_g depression of the composites containing nano-AlN was related to the aggregation of nano-

AlN and voids. Compared with micro-AlN, the increase in the dynamic modulus and the decrease in CTE for the nano-AlN-filled composites indicated that the greater interfacial area between nano-AlN and the epoxy matrix effectively hindered deformation of the epoxy, although the interaction between them was weak in some regions because of the aggregation of nano-AlN and voids. In addition, the decrease in the crosslink density of the epoxy matrix also resulted in T_g depression and a change in CTE and E' of post-T_g.

5. At a fixed AlN content of 10 wt %, micro-AlN plus nano-AlN with different weight ratios was filled into the epoxy. When the weight ratio of nano-AlN in a combination of micro-AlN plus nano-AlN was relatively small (0.17–0.33), high T_g and low E' were observed. This may have been related to the best packing efficiency at that weight ratio when the bimodal filler was used. This best packing efficiency was more clearly observed at high AlN content.

References

1. Ha, S. R.; Ryu, S. H.; Park, S. J.; Rhee, K. Y. Mater Sci Eng A 2007, 448, 264.
2. Musumeci, A. W.; Silva, G. G.; Liu, J. W.; Martens, W. N.; Waclawik, E. R. Polymer 2007, 48, 1667.
3. Shi, Q. A.; Wang, L.; Yu, H. J.; Jiang, S.; Zhao, Z. R.; Dong, X. C. Macromol Mater Eng 2006, 291, 53.
4. Wetzel, B.; Haupert, F.; Zhang, M. Q. Compos Sci Technol 2003, 63, 2055.
5. Kim, Y. A.; Kamio, S.; Tajiri, T.; Hayashi, T.; Song, S. M.; Endo, M.; Terrones, M.; Dresselhaus, M. S. Appl Phys Lett 2007, 90, 93125.
6. Chang, T. E.; Kisliuk, A.; Rhodes, S. M.; Brittain, W. J.; Sokolov, A. P. Polymer 2006, 47, 7740.
7. Yung, K. C.; Wu, J.; Yue, T. M.; Xie, C. S. J Compos Mater 2006, 40, 567.
8. Bleach, N. C.; Nazhat, S. N.; Tanner, K. E.; Kellomaki, M.; Tormala, P. Biomaterials 2002, 23, 1579.
9. Goyanes, S. N.; Konig, P. G.; Marconi, J. D. J Appl Polym Sci 2003, 88, 883.
10. Park, S. J.; Jin, F. L.; Lee, C. J. Mater Sci Eng A 2005, 402, 335.
11. Goyal, R. K.; Tiwari, A. N.; Mulik, U. P.; Negi, Y. S. Compos A 2007, 38, 516.
12. Hu, Y. H.; Chen, C. Y.; Wang, C. C. Polym Degrad Stab 2004, 84, 545.
13. Zhou, Y. X.; Pervin, F.; Rangari, V. K.; Jeelani, S. Mater Sci Eng A 2006, 426, 221.
14. Basara, G.; Yilmazer, U.; Bayram, G. J Appl Polym Sci 2005, 98, 1081.
15. Choi, Y. K.; Sugimoto, K.; Song, S. M.; Gotoh, Y.; Ohkoshi, Y.; Endo, M. Carbon 2005, 43, 2199.
16. Ash, B. J.; Siegel, R. W.; Schadler, L. S. J Polym Sci Part B: Polym Phys 2004, 42, 4371.
17. Miyagawa, H.; Drzal, L. T. Polymer 2004, 45, 5163.
18. Preghenella, M.; Pegoretti, A.; Migliaresi, C. Polymer 2005, 46, 12065.
19. Huang, Y. Q.; Jiang, S. L.; Wu, L. B.; Hua, Y. Q. Polym Test 2004, 23, 9.
20. Sandler, J.; Werner, P.; Shaffer, M. S. P.; Demchuk, V.; Altstadt, V.; Windle, A. H. Compos A 2002, 33, 1033.
21. Sun, Y. Y.; Zhang, Z. Q.; Moon, K. S.; Wong, C. P. J Polym Sci Part B: Polym Phys 2004, 42, 3849.
22. Xiong, M. N.; Gu, G. X.; You, B.; Wu, L. M. J Appl Polym Sci 2003, 90, 1923.
23. Bae, J. W.; Kim, W.; Cho, S. H.; Lee, S. H. J Mater Sci 2000, 35, 5907.
24. Ishida, H.; Rimdusit, S. Thermochim Acta 1998, 320, 177.
25. Xu, J. W.; Moon, K. S.; Tison, C.; Wong, C. P. IEEE Trans Adv Pack 2006, 29, 295.
26. Kwon, S. C.; Adachi, T.; Araki, W.; Yamaji, A. Acta Mater 2006, 54, 3369.
27. Wong, C. P.; Bollampally, R. S. J Appl Polym Sci 1999, 74, 3396.
28. Kim, W.; Bae, J. W.; Choi, I. D.; Kim, Y. S. Polym Eng Sci 1999, 39, 756.
29. Yung, K. C.; Zhu, B. L.; Wu, J.; Yue, T. M.; Xie, C. S. J Polym Sci Part B: Polym Phys 2007, 45, 1662.
30. Greenwood, R.; Luckham, P. F.; Gregory, T. J Colloid Interface Sci 1997, 191, 11.
31. Peters, A. C. I. A.; Overbeek, G. C.; Annable, T. Prog Org Coat 2000, 38, 137.
32. Nunez, L.; Nunez, M. R.; Villanueva, M.; Castro, A.; Rial, B. J Appl Polym Sci 2002, 85, 366.
33. Fambri, L.; Kesenci, K.; Migliaresi, C. Polym Compos 2003, 24, 100.
34. Chen, D. Z.; Tang, C. Y.; Chan, K. C.; Tsui, C. P.; Yu, P. H. F.; Leung, M. C. P.; Uskokovic, P. S. Compos Sci Technol 2007, 67, 1617.
35. Kang, S.; Hong, S. I.; Choe, C. R.; Park, M.; Rim, S.; Kim, J. Polymer 2001, 42, 879.
36. Ash, B. J.; Schadler, L. S.; Siegel, R. W. Mater Lett 2002, 55, 83.
37. Liang, J. Z.; Li, R. K. Y.; Tjong, S. C. Polym Int 1999, 48, 1068.
38. Miyagawa, H.; Rich, M. J.; Drzal, L. T. J Polym Sci Part B: Polym Phys 2004, 42, 4384.
39. Guan, C.; Lu, C. L.; Liu, Y. F.; Yang, B. J Appl Polym Sci 2006, 102, 1631.